ESTIMATION OF THE LIDAR OVERLAP FUNCTION BY NON-LINEAR REGRESSION

A. C. Povey[1], **R. G. Grainger**[1], **D. M. Peters**[1], **J. L. Agnew**[2], **and D. Rees**[3]

[1]*University of Oxford, Atmospheric, Oceanic, and Planetary Physics, Clarendon Laboratory, Parks Road, Oxford, OX1 3PU, United Kingdom, povey@atm.ox.ac.uk*
[2]*STFC Rutherford Appleton Laboratory, Harwell, Oxford, OX11 0QX, United Kingdom*
[3]*Hovemere Ltd., Tonbridge, TN9 1RF, United Kingdom, drees@hovemere.com*

ABSTRACT

The overlap function of a Raman channel for a lidar system is retrieved by non-linear regression using an analytic description of the optical system and a simple model for the extinction profile, constrained by aerosol optical thickness. Considering simulated data, the scheme is successful even where the aerosol profile deviates significantly from the simple model assumed. Application to real data is found to reduce by a factor of 1.4 – 2.0 the root-mean-square difference between the attenuated backscatter coefficient as measured by the calibrated instrument and a commercial instrument.

1. INTRODUCTION

A lidar's overlap function describes the efficiency with which light is coupled into its detectors as a function of height, dependent on overlap of the laser-illuminated volume with the system's field-of-view (FOV) and losses in the optical system. [1, 2] This limits the accuracy with which lidar can be used to investigate the planetary boundary layer (PBL), where aerosol is both most abundant and most variable. Further, many methods of lidar analysis are designed to only consider regions where the overlap function is constant and can incur significant errors if regions where it is not constant are considered.

The Robust And Compact Environmental Lidar (RACHEL) was developed by Hovemere Ltd. as a cost-effective and portable Raman lidar system for unattended monitoring of pollution by day and night. The prototype system was deployed at the NERC Chilbolton Facility for Atmospheric and Radio Research (CFARR) in southern England during Spring 2010. Due to a series of minor faults, the laser was operating at significantly less than its full power and had to be adjusted repeatedly in the field, such that the usually assumed analytic form could not be used. The low signal-to-noise ratio (SNR) of the data prevented iterative methods [3, 4] from converging to sufficiently smooth solutions to be useful. Further, the large, inhomogeneous aerosol loading ruled out integrating the signal over longer time periods to increase the SNR. A new method was sought to produce the best estimate of the overlap function possible under these challenging conditions.

Non-linear regression provides a framework to combine these noisy lidar profiles with other information about the system and atmosphere, such as an analytic model of the overlap function or aerosol optical thickness, to produce an estimate of the overlap function that makes optimal use of all the information available. The retrieved overlap function is then used to produce a simple lidar product, which is compared to independent observations as an initial validation. This extended abstract should serve as a brief outline for a paper of the same title currently under review for publication in *Applied Optics*.

2. METHOD

2.1 Optimal estimation

Optimal estimation is a non-linear regression scheme with rigorous incorporation of any prior information about the state of the system. [5] It solves for $\mathbf{x}$ the inverse problem,

$$\mathbf{y} = \mathbf{F}(\mathbf{x}, \mathbf{b}) + \varepsilon, \tag{1}$$

where $\mathbf{y}$ describes a set of measurements with noise ε; the state of the observing system and atmosphere are summarised by unknown parameters $\mathbf{x}$ and known parameters $\mathbf{b}$; and the forward model $\mathbf{F}$ translates this state into a simulated measurement.

If the uncertainty in the measurements is described by a covariance matrix $\mathbf{S}_\varepsilon$ and the probability density function for all variables is approximated as Gaussian, the probability that the system is in a state $\mathbf{x}$ given the measurement $\mathbf{y}$ can be expressed as,

$$
\begin{aligned}
-2\ln P(\mathbf{x}|\mathbf{y}) \;=\; & [\mathbf{y} - \mathbf{F}(\mathbf{x},\mathbf{b})]^T \mathbf{S}_\varepsilon^{-1} [\mathbf{y} - \mathbf{F}(\mathbf{x},\mathbf{b})] \\
& + [\mathbf{x} - \mathbf{x}_a]^T \mathbf{S}_a^{-1} [\mathbf{x} - \mathbf{x}_a] + c,
\end{aligned}
\tag{2}
$$

where c is a constant. The second term above incorporates any information we may have about the system before making the measurement through an *a priori* state $\mathbf{x}_a$ with covariance matrix $\mathbf{S}_a$. These could, for example, describe a climatological mean state or expected correlations in some quantity with height due to vertical mixing.

It is then shown in [5] that the iteration,

$$
\begin{aligned}
\mathbf{x}_{i+1} \;=\; & \mathbf{x}_i + [(1+\Gamma_i)\mathbf{S}_a^{-1} + \mathbf{K}_i^T \mathbf{S}_\varepsilon^{-1} \mathbf{K}_i]^{-1} \\
& \{\mathbf{K}_i^T \mathbf{S}_\varepsilon^{-1} [\mathbf{y} - \mathbf{F}(\mathbf{x}_i, \mathbf{b})] - \mathbf{S}_a^{-1}(\mathbf{x}_i - \mathbf{x}_a)\},
\end{aligned}
\tag{3}
$$

converges to the minimum of (2) — the most likely state. Here, $\mathbf{K}_i = \nabla_{\mathbf{x}} \mathbf{F}(\mathbf{x}_i, \mathbf{b})$ and the covariance of that state is,

$$\mathbf{S}_{\mathbf{x}} = (\mathbf{K}^T \mathbf{S}_\varepsilon^{-1} \mathbf{K} + \mathbf{S}_a^{-1})^{-1}. \tag{4}$$

General practice is that after an iteration, if the value of the cost function (2) has increased, the scaling factor Γ_i

Table 1. RACHEL system specification

Parameter	Value
Laser type	Nd-YAG
Emitted wavelength	354.7 nm
Pulse rate	20 Hz
Average pulse energy	45 mJ
Beam radius, R_L	17.5 mm
Beam divergence, ϕ_L	0.3 mrad
Telescope model	Meade LXD-75
Primary mirror radius, R_T	101.5 mm
Secondary mirror radius, R_o	37.5 mm
Fibre radius, R_p	0.2 mm
Focal length, f	2.0 m
Resolution	10.5 m

is increased by a factor of ten. Otherwise, it is reduced by a factor of two. Iteration ceases when either the cost function or all elements of the state vector change by less than some threshold after a step.

2.2 Application to lidar

The most common model for the response of a lidar to Raman scattering from particles is, [1, 2]

$$
\begin{aligned}
E_{ra}(r) &= E_0 \, C_{ra} \, r^{-2} A(r) N_X(r) \\
&\times \exp\left[-\int_0^r \alpha_m(\lambda_L, r') + \alpha_a(\lambda_L, r') \right. \\
&\left. + \alpha_m(\lambda_X, r') + \alpha_a(\lambda_X, r') \, dr' \right], \quad (5)
\end{aligned}
$$

where $E_{ra}(r)$ is the energy observed from a range r; $\beta(\lambda, r)$ is the backscattering coefficient; $\alpha(\lambda, r)$ is the extinction coefficient; the subscripts m and a denote molecular and aerosol scattering; λ_L and λ_X are the wavelengths of the laser beam and Raman scattered radiation; E_0 is the energy of the laser pulse; $N_X(r)$ is the number density of the scattering species; and C_{ra} is a constant.

For the purpose of estimating the overlap function, the measurement **y** will be the values of E_{ra} over some suitable range; the state **x** will be the values of C_{ra}, $A(r)$, and α_a over the same range; and the remaining variables are known from other measurements (such as a standard atmosphere) and so form **b**. To further constrain the problem, model analytic forms for $A(r)$ and α_a are introduced such that these profiles can be expressed in terms of a few unknown parameters.

Such a formulation for $A(r)$ was proposed in [6] (not outlined here for brevity). This presented the overlap function as an integral over the overlap of two circles — the assumed circular, continuous beam and the telescope's FOV. It neglects the effects of any components after the telescope and any variations in the beam profile. Some rearrangement of the form originally presented was made to improve accuracy and stability of the integration.

It is then hypothesised from observations [7, 8, 9] that stable PBLs can be approximated as having constant extinction up to some height z_0 (which is not necessarily the top of the PBL) and a rapid exponential decay above that over a scale height H. This profile can then be con-

strained by observations of the atmosphere, such as measurement of the aerosol optical thickness, χ, with a sun photometer. This profile can be written as (see fig. 1(a)),

$$
\int_0^z \alpha_a(\lambda_L, r') \, dr' = \left\{ \begin{array}{ll} \frac{\chi}{H+z_0} z, & z < z_0; \\ \frac{\chi}{H+z_0} \left[z_0 + H\left(1 - \exp\frac{z_0 - z}{H}\right)\right], & z \geq z_0. \end{array} \right. \tag{6}
$$

3. SIMULATION

The behaviour of the retrieval scheme was investigated through the use of data simulated for the RACHEL platform (table 1). Such simulations are easily produced with the forward model, with four alignments of the system considered to highlight the expected range of states.

As shown in fig. 2, retrievals for all four cases demonstrate a high quality fit, with costs in the expected range. There is a slight tendency towards underestimation with height, most pronounced in curve $\times$. This is to be expected as this model has the lowest magnitude. That being directly proportional to the number of photons observed, the SNR will be lower for this profile, corresponding to a lower information content in the retrieval. When the integration time of this profile is increased, the fit is found to be equivalent to the others.

To investigate the suitability of the idealised extinction profile, a variety of perturbations were added, shown in fig. 1(b–c), and simulated using a well-aligned model.
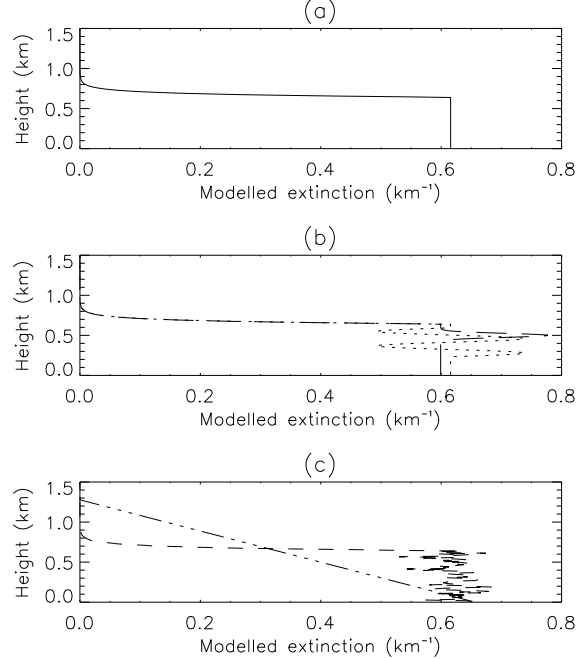

Figure 1. Aerosol extinction profiles used for simulating data. All have $\chi = 0.4$ at 355 nm. (a) Unperturbed model profile, where extinction is constant to 640 m and decreases exponentially above that; (b) Addition of a Gaussian peak (dash) or sinusoidal variations (dot); (c) Addition of normally-distributed multiplicative noise (short dashes) or a linear decrease in extinction (dot-dash).
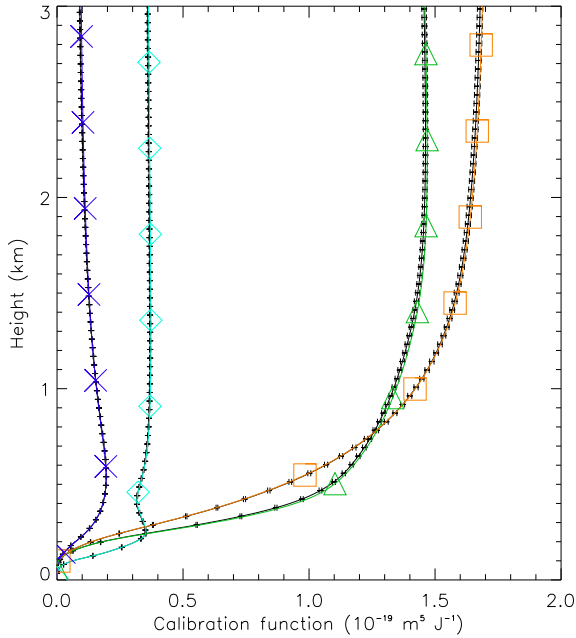
Figure 2. Retrieved calibration function, $C_{ra}A(r)$, for four different model alignments (black) with errors derived from eqn. (4). The true profile is plotted in colour.

All are constructed to have an equal χ of 0.4 at 355 nm. In three cases, the retrieved profile was consistent with that used for simulation and in the case of a linear decrease in extinction with height, the retrieval is accurate to within 5 % despite the significant difference in extinction profile, though this difference is greater than the predicted error. These profiles also demonstrated a significant degeneracy in the model, with different sets of parameters producing practically identical overlap functions. As such, it is important to evaluate the success of any retrieval against the calibration function and its error and not the individual parameters, which may not be physically meaningful.

The impact of a different beam profile on the retrieval was also investigated. The overlap function was recalculated with a Gaussian beam profile for each of the four model states. The retrieval was then applied assuming a continuous profile. The results vary, with discrepancies of up to 10 % in the region 200 – 1000 m, where the overlap of the beam and FOV is most rapidly changing and the beam profile is most important. However, such cases are indicated by a large cost for the retrieval, and so can be identified and rejected.

4. APPLICATION

The retrieval was then applied to real data. Ideally, observations at night would be used as these have a higher SNR and, sufficiently long after sunset, the PBL will generally be stable. However, as it was not possible to measure χ at night, a balance was sought by considering early morning and dawn of days that showed minimal variation in χ within an hour of sunrise.

The retrieved calibration function from one morning's observations is plotted in fig. 3(a). For comparison, a simple arithmetic inversion of eqn. (5) is also shown (calculated by correcting the measurements for range, background, molecular scattering, and the *a priori* aerosol profile). Firstly, the overlap function tends smoothly to a constant value with height, indicating RACHEL was well aligned at this time. The retrieved profile is slightly
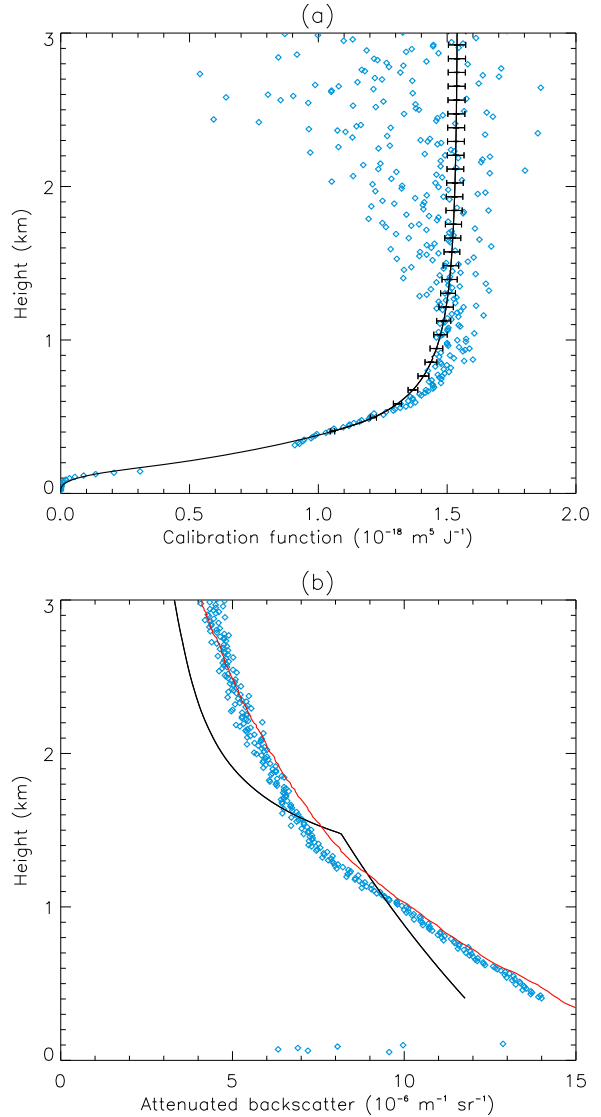

Figure 3. (a) The retrieved calibration function with errors. Plotted as points is an arithmetic inversion of the measurement, eqn. (5), with the *a priori* extinction profile. Measurements beyond the reasonably linear range of the detectors are not plotted and were not used in the retrieval. (b) The attenuated backscatter coefficient at 355 nm for the retrieved aerosol profile (black), the elastic profile corrected with the retrieved overlap function (blue), and as reported independently by an EZ lidar at the same site (red). A lidar ratio of 15 was chosen to give consistency between the three signals above 6 km.

smaller from 0.5 – 1 km than would be expected from the data without retrieval as the retrieved scale height is greater than initially guessed. It is further evident that the retrieval is returning larger errors than observed in the simulated data. The reason for this is clear from the broad scatter of data points above 1 km. The ability to fit a physically consistent function regardless is one of optimal estimation's strengths.

The validity of the retrieved extinction profile can be explored through use of the elastic channel. In particular, if a constant lidar ratio is assumed, the attenuated backscatter coefficient,

$$\beta^*(r) \quad = \quad \frac{E_{\mathrm{el}}(r)\,r^2}{C_{\mathrm{el}}E_0 A(r)} \exp\left[2\int_0^r \alpha_m(\lambda_L, r')\,\mathrm{d}r'\right] \quad (7)$$

$$\equiv \quad \frac{\beta_m(\lambda_L, r) + \beta_a(\lambda_L, r)}{\exp\left[2\int_0^r \alpha_a(\lambda_L, r')\,\mathrm{d}r'\right]}, \quad (8)$$

can be calculated for the elastic channel and compared to that from direct substitution of the retrieved α_a into eqn. (8). This is presented in fig. 3(b), with the retrieved profile in black and the elastic data in blue . In addition, plotted in red is the β^* published by CFARR from a Leosphere EZ lidar operated continuously at the site, evaluated using Leosphere's commercial algorithm.

We can see that in this case, the retrieved α_a is reasonable up to 1.5 km, but then underestimates the scale height. However, the fairly good correspondence between the published β^* and that determined from RACHEL's elastic channel (the RMS deviation between them reduces from $2.4 \times 10^{-5}\,\mathrm{m}^{-1}\,\mathrm{sr}^{-1}$ without overlap correction to 1.4×10^{-5} with it) gives confidence that despite the extinction profile, the retrieved correction is useful. The difference in α_a may be due to a change in the lidar ratio between the PBL and free troposphere.

5. CONCLUSIONS

An optimal estimation scheme has been proposed for the retrieval of the overlap function of a Raman channel of a lidar system. The retrieval scheme was successful in retrieving overlap functions from simulated data, with various perturbations to the assumed aerosol profile found to not significantly affect the result. The use of a Gaussian beam profile was found to influence the retrieval in some circumstances, but these failures were indicated by high costs and so can be rejected.

The retrieval was then applied to measurements with the RACHEL system. This was found to be more consistent with independent observations than without the overlap correction by a factor of 1.4 – 2.0. The retrieved extinction profiles, though functional, were clearly only approximations to the truth. It is likely that a model of the extinction profile with more degrees of freedom could improve the technique in future.

Practically, the retrieved overlap function will be used within some algorithm to derive the extinction and backscatter. For a Klett-Fernald scheme, as the overlap function is effectively a multiplicative correction, it will simply add to the fractional error in the backscatter coefficient. For the conditions considered in Section 4, this varies from about 2 % when the system is well aligned, which is slightly better that that expected from existing techniques of determining the overlap function, to over 10 % when it isn't well aligned, which would be the dominant source of error in the retrieval, though this was in part due to the lower SNR of the data used in the retrieval (not presented here).

The impact of this error on a Raman lidar scheme is more subtle as there the correction is to the derivative of the overlap function. In its current form, the dominant error in this derivative is from numerical integration and can be over 100 % in certain cases. However, if an analytic form of the derivative is found, the errors should be equivalent to those introduced into the single-channel scheme. This is an aim for the near future.

REFERENCES

[1] Measures, R. M., 1992: *Lidar Remote Sensing: Fundamentals and Applications*. Krieger Publishing Company.

[2] Fujii, T., T. Fukuchi, 2005: *Laser remote sensing*. Taylor and Francis.

[3] Wandinger, U., A. Ansmann, 2002: Experimental determination of the lidar overlap profile with Raman lidar. *Applied Optics*, **41**, pp. 511–514.

[4] Guerrero-Rascado, J. L. *et al.*, 2010: Infrared lidar overlap function: an experimental determination. *Optics Express*, **18**, pp. 20350–20359.

[5] Rodgers, C. D., 2000: *Inverse methods for atmospheric sounding: Theory and practice*, World Scientific.

[6] Halldórsson, T., J. Langerholc, 1978: Geometrical form factors for the lidar function. *Applied Optics*, **17**, pp. 240–244.

[7] Steyn, D. G., M. Baldi, R. M. Hoff, 1999: The detection of mixed layer depth and entrainment zone thickness from lidar backscatter profiles. *Journal of Atmospheric and Oceanic Technology*, **16**, pp. 953–959.

[8] He, Q. S. *et al.*, 2008: Analysis of aerosol vertical distribution and variability in Hong Kong. *JGR — Atmospheres*, **113**, p. 13.

[9] Wiegner, M. *et al.*, 2006: Mixing layer height over Munich, Germany: Variability and comparisons of different methodologies. *JGR — Atmospheres*, **111**, p. 17.